# SUPPLEMENTARY MATERIAL FOR

# Biofilm Inhibitory Abscisic Acid Derivatives from the Plant-Associated Dothideomycete Fungus, *Roussoella* sp.

**Chayanard Phukhamsakda [1], Allan Patrick G. Macabeo [2,3], Kamila Tomoko Yuyama [2], Kevin David Hyde [1] and Marc Stadler [2,*]**

[1] Center of Excellence in Fungal Research, Mae Fah Luang University, Chiang Rai, 57100 Thailand; chayanard91@gmail.com; kdhyde3@gmail.com
[2] Department of Microbial Drugs, Helmholtz Centre for Infection Research and German Centre for Infection Research (DZIF), partner site Hannover/Braunschweig, Inhoffenstrasse 7, 38124, Braunschweig, Germany; kamilatomoko@gmail.com
[3] Laboratory for Organic Reactivity, Discovery and Synthesis (LORDS), Research Center for the Natural and Applied Sciences, University of Santo Tomas, 1015 Manila, Philippines; agmacabeo@ust.edu.ph

***** Correspondence: Marc.Stadler@helmholtz-hzi.de; Tel.: +49-531-6181-4240.

## LIST OF SUPPORTING INFORMATION

**S1.** Morphological features and molecular phylogenetic

**S1.1** Identification of *Roussoella sp.* MFLUCC 17-2059

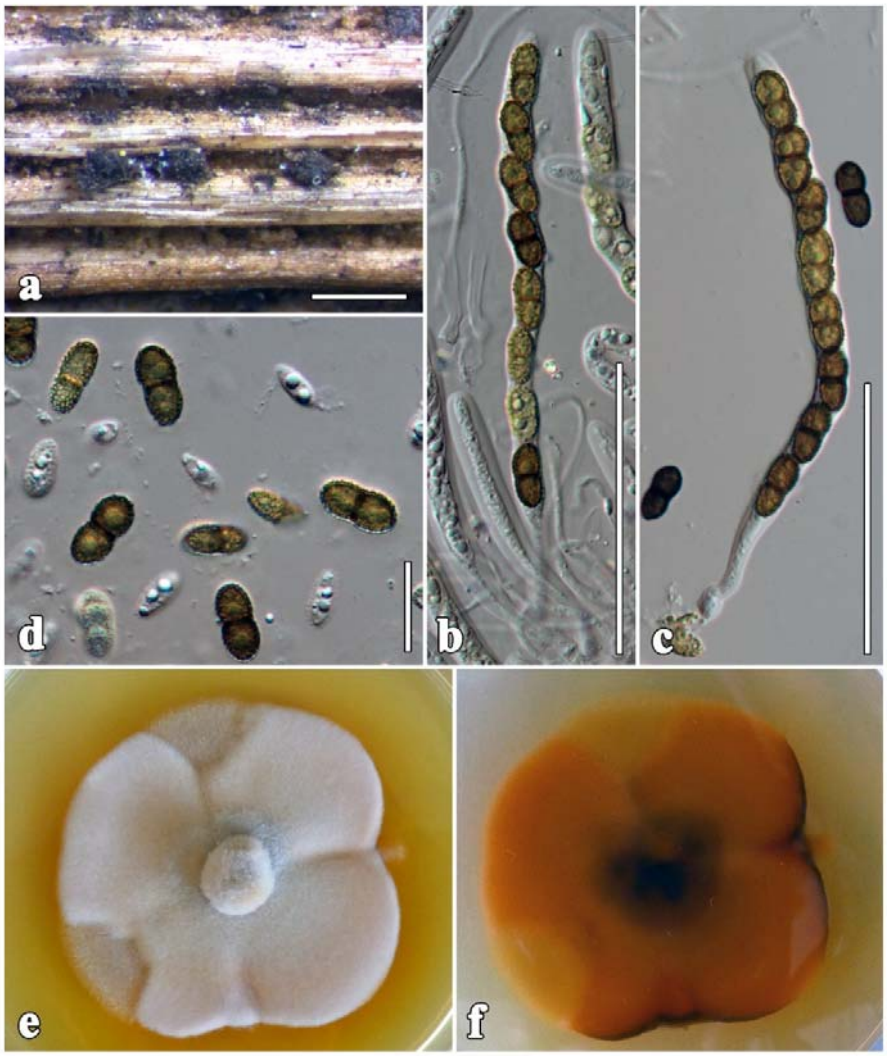


**Figure S1.1** *Roussoella sp.* MFLUCC 17-2059 **a** Appearance of ascomata on host surface **b-c** Asci **d** Ascospores e-f Culture characters on YMG agar. **Scale bars:** a = 500 *µm*, b-c = 50 *µm*, d = 10 *µm.*

Material examined: Dried branched *Clematis subumbellata* (Ranunculaceae), Thailand, living culture = MFLUCC 17-2059.

**S1.2** Phylogenetic study

The aligned ITS and TEF-1α sequences were concatenated to generate multigenes alignment phylogenetic tree. Maximum Likelihood were constructed by using CIPRES webportal online tools (Miller et al. 2010), including 1,000 bootstrap replicates. According to the data set combining the morphological features and phylogenetic analysis, the fungus was identified as *Roussoellaceae* member.

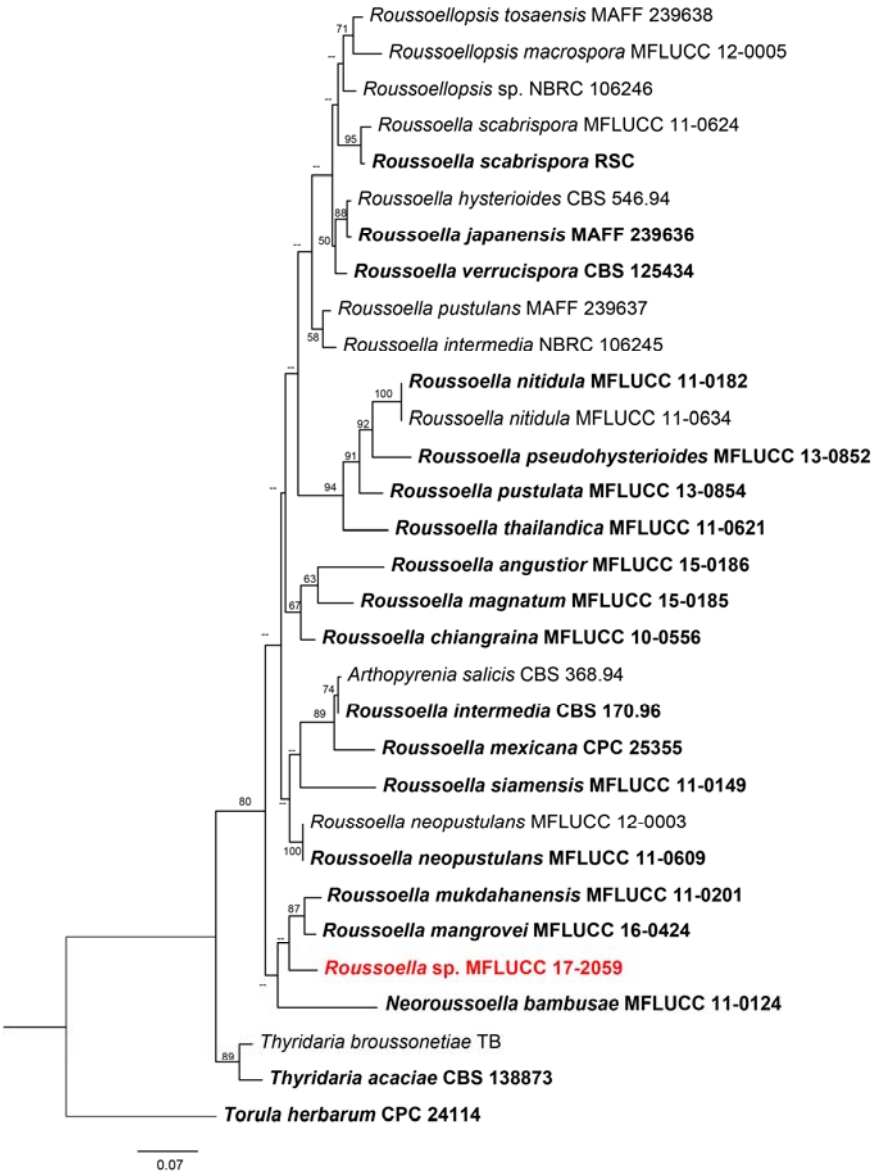


**Fig S1.2.** Phylogenetic tree of the combined data set of two markers, RAxML (ITS and TEF-1α). The strain produced secondary metabolites in this study is marked in red.

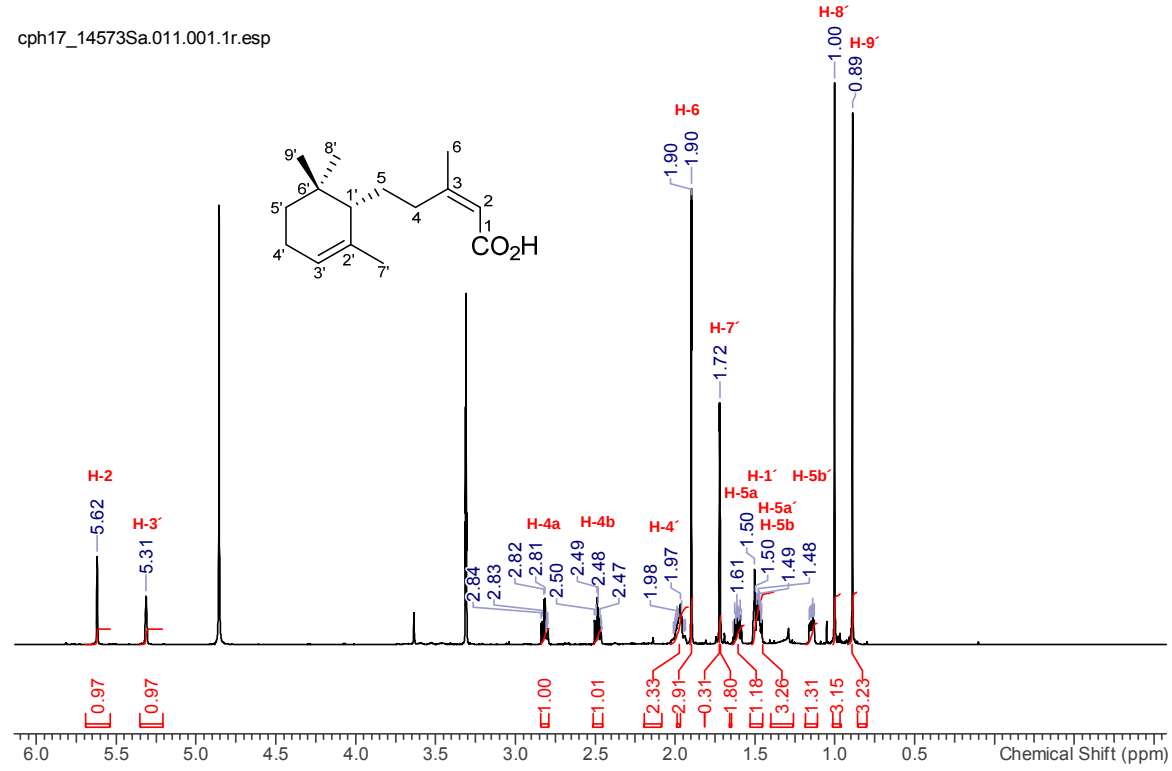


**S2.** $^{1}$H NMR spectrum (MeOH-$d_4$, 700 MHz) of roussoellenic acid (**1**).

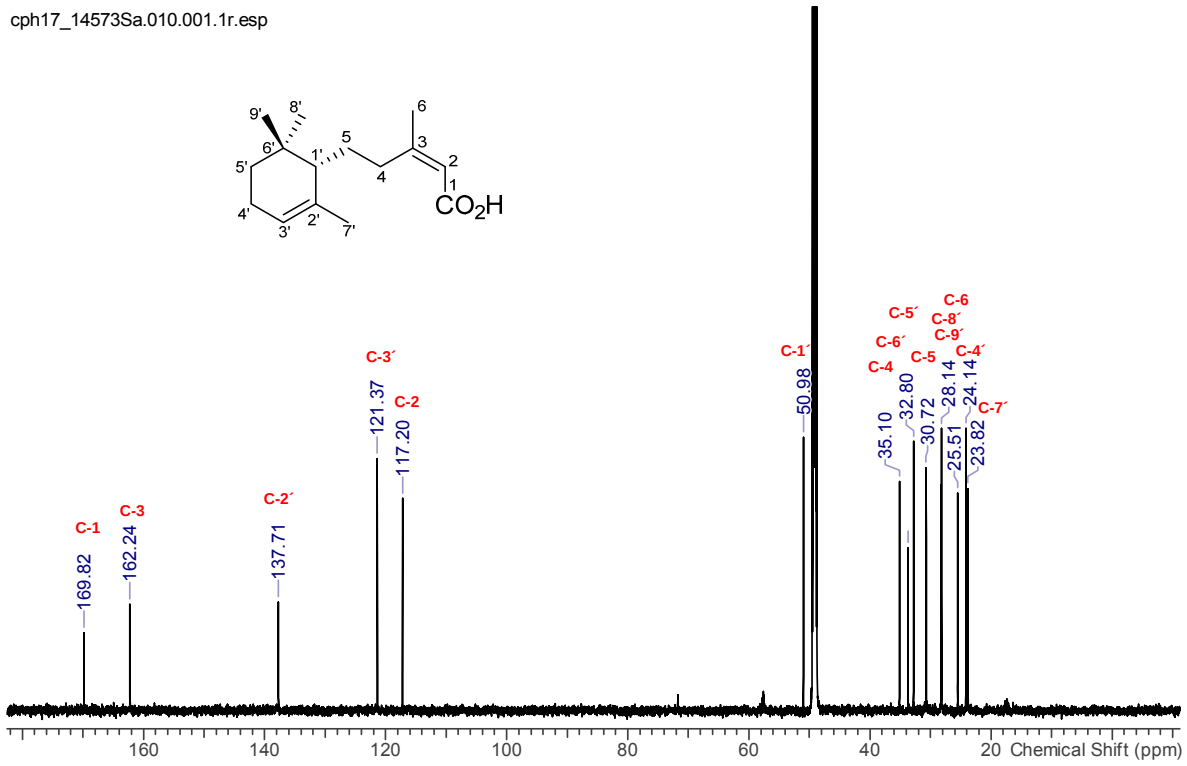


**S3.** $^{13}$C NMR spectrum (MeOH-$d_4$, 175 MHz) of roussoellenic acid (**1**).

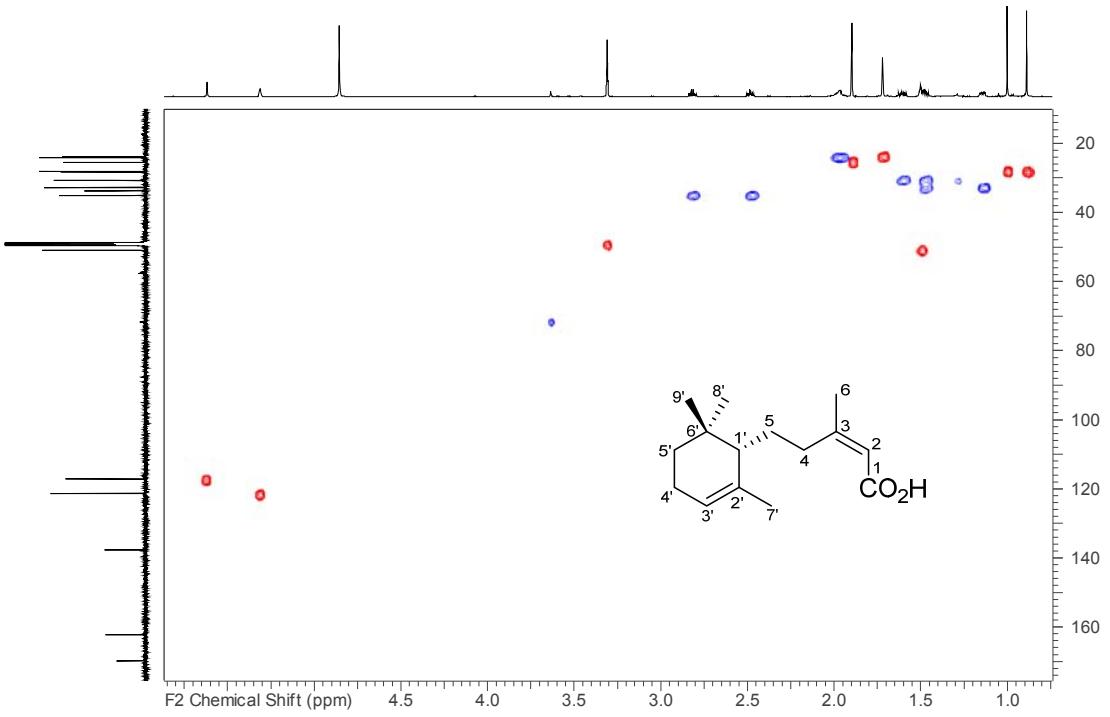


**S4.** HSQC-DEPT* edited spectrum of roussoellenic acid (**1**).

* blue crosspeak – $CH_2$; red crosspeak – $CH/CH_3$

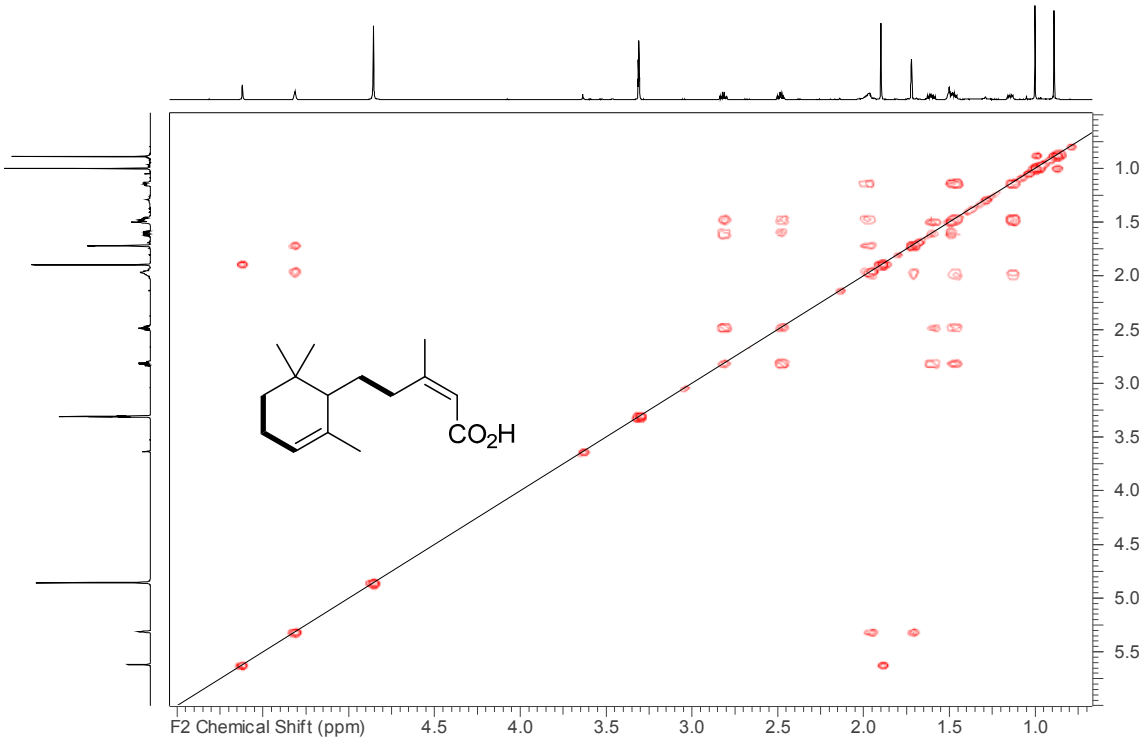


**S5.** COSY spectrum of l roussoellenic acid (**1**).

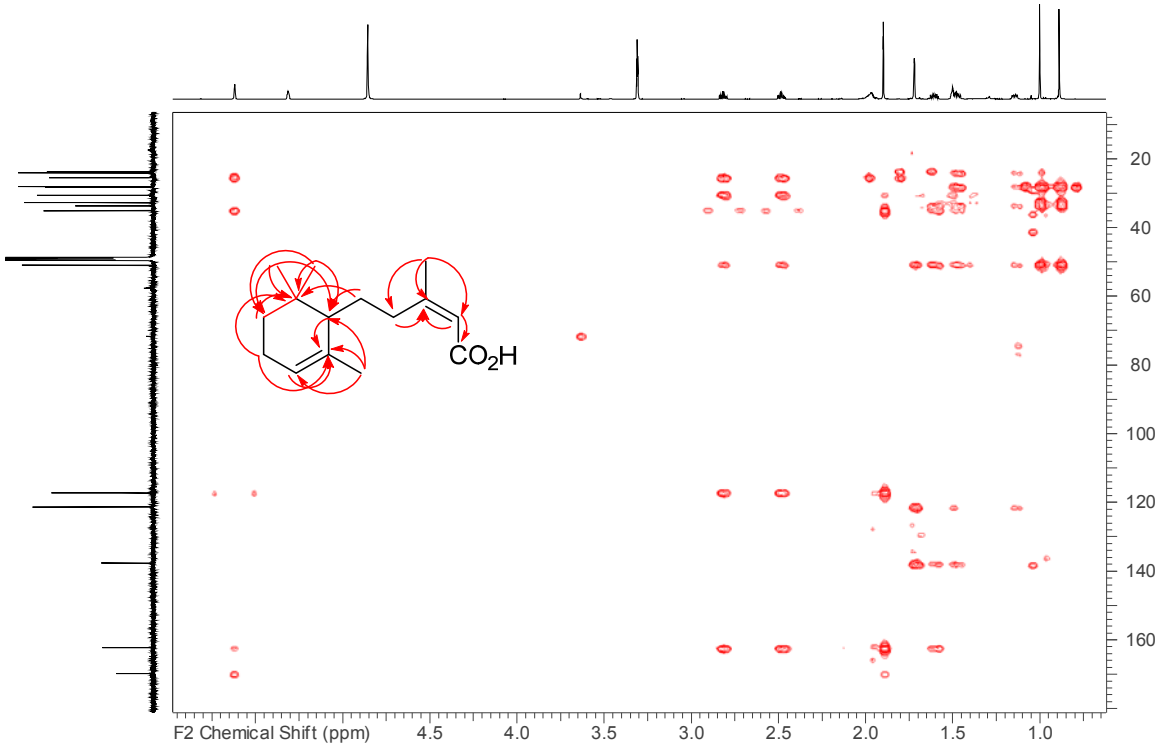


**S6.** HMBC spectrum of roussoellenic acid (**1**).

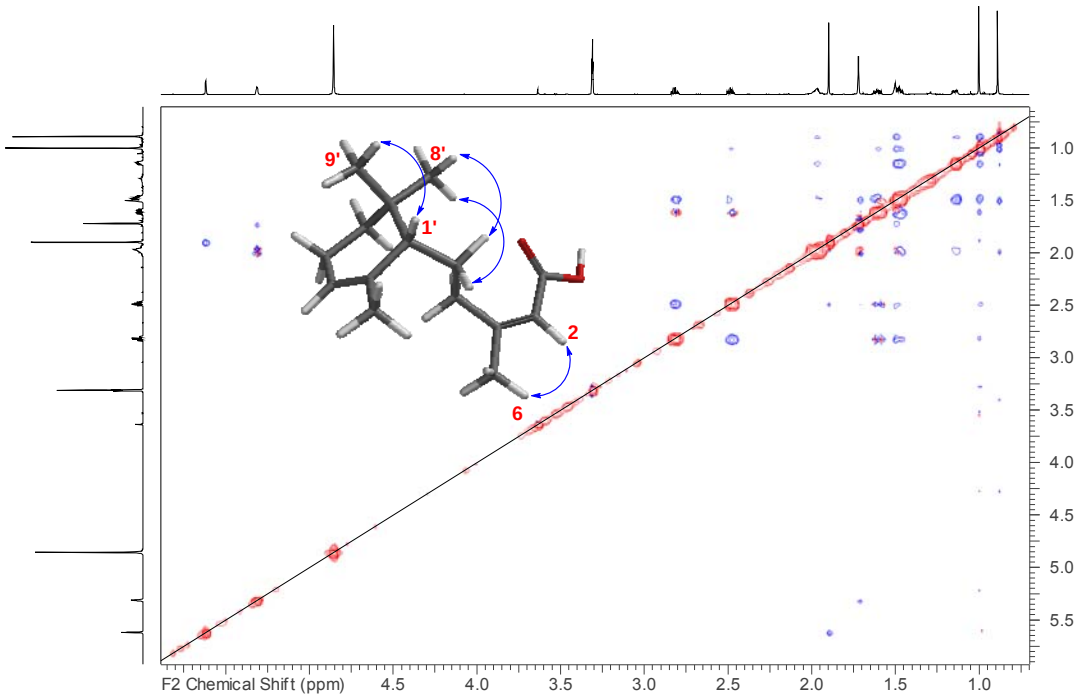


**S7.** NOESY spectrum of roussoellenic acid (**1**).

* NOE correlations are indicated by blue off-diagonal peaks.

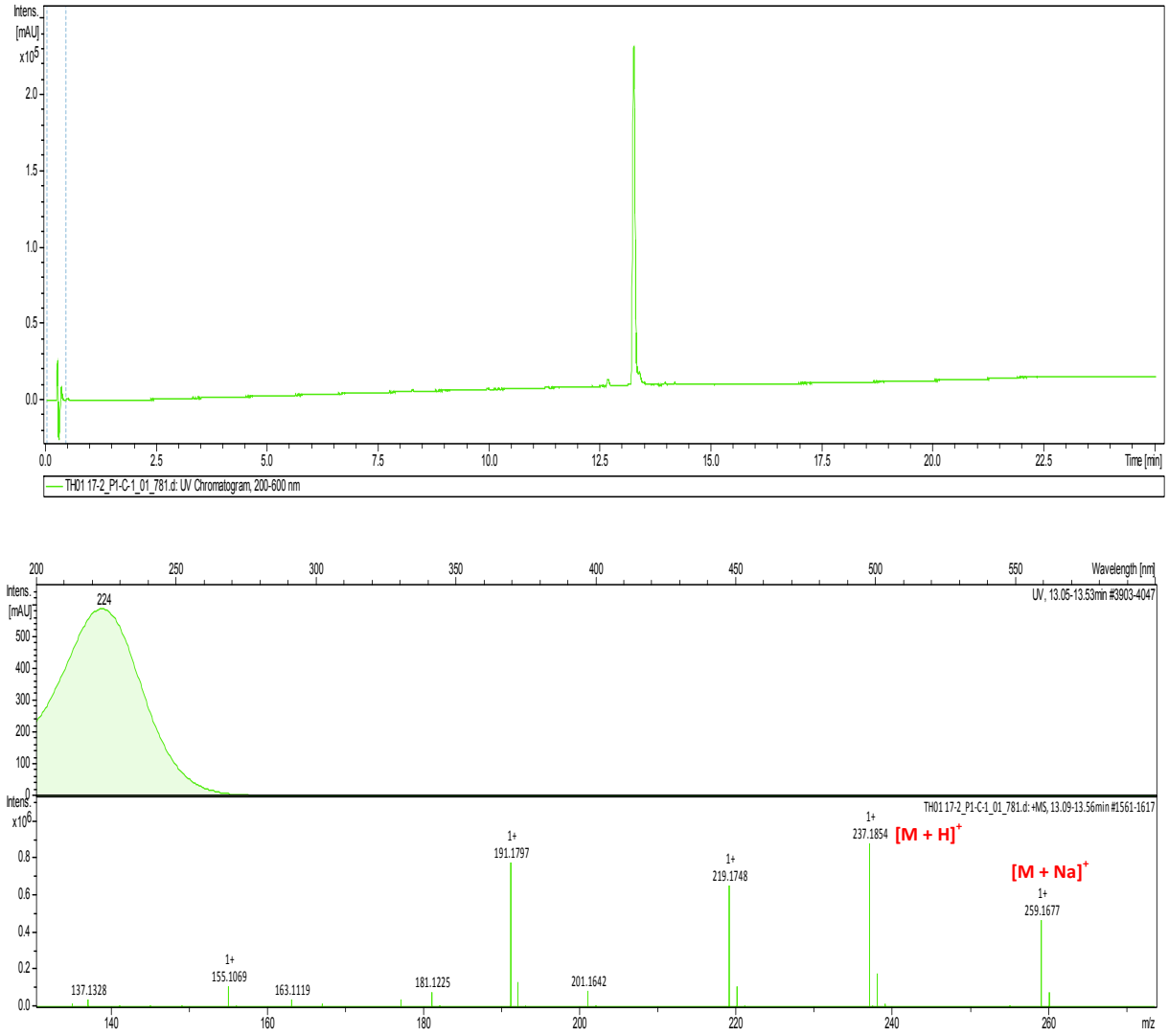


**S8.** LC-DAD-HR-ESIMS spectrum of roussoellenic acid (**1**).

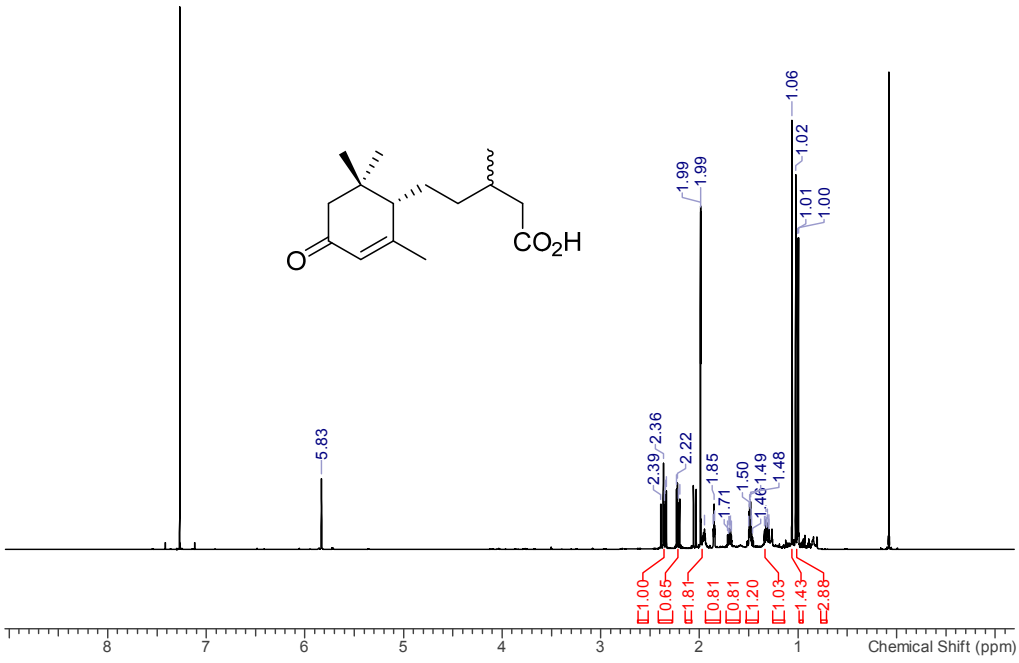


**S9.** $^{1}$H NMR spectrum ($CDCl_3$, 700 MHz) of pestabacillin B (**2**).

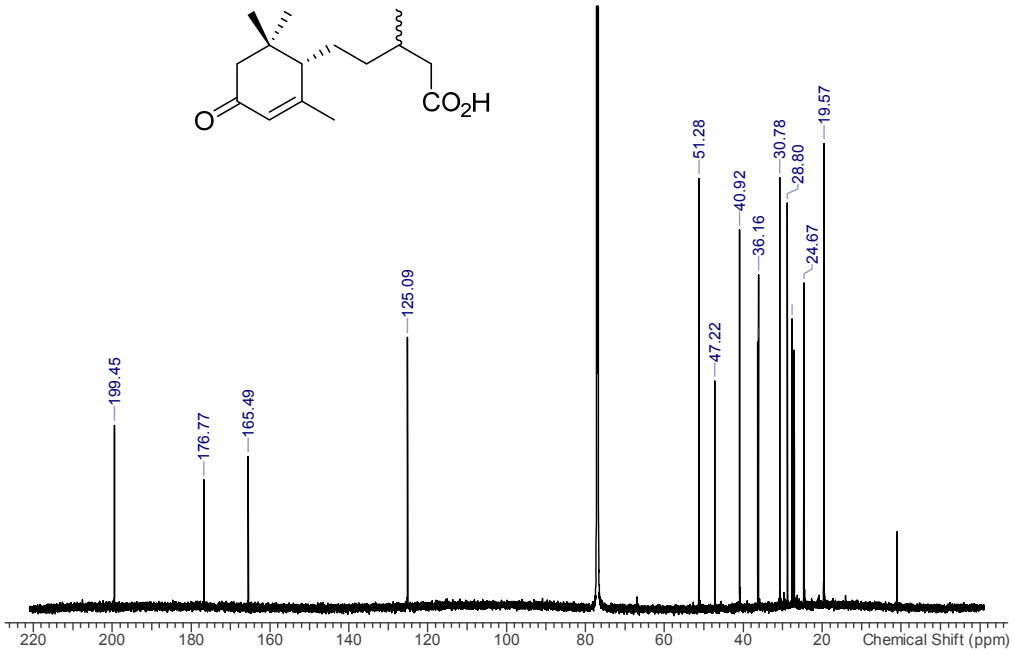


**S10.** $^{13}$C NMR spectrum ($CDCl_3$, 175 MHz) of pestabacillin B (**2**).

Liu, S.; Dai, H.; Heering, C.; Jania, C.; Lin, W.; Liu, Z.; Proksch, P. *Tetrahedron Lett.* **2017**, *58,* 257-261.

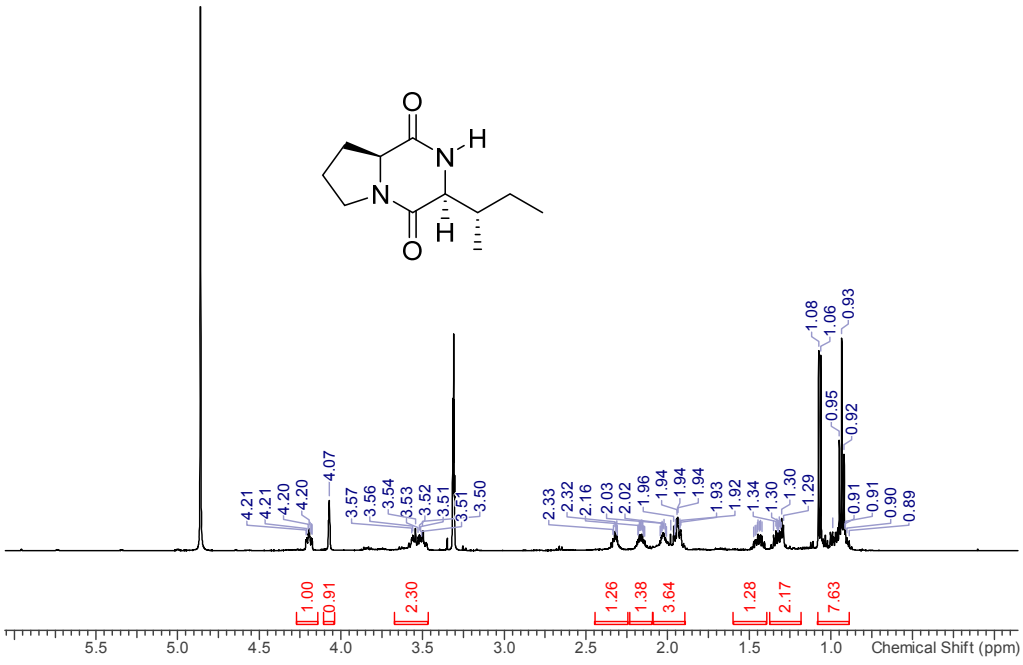


**S11.** $^{1}$H NMR spectrum (MeOH-$d_4$, 700 MHz) of *cyclo*(*S*-Pro-*S*-Ile) (**3**).

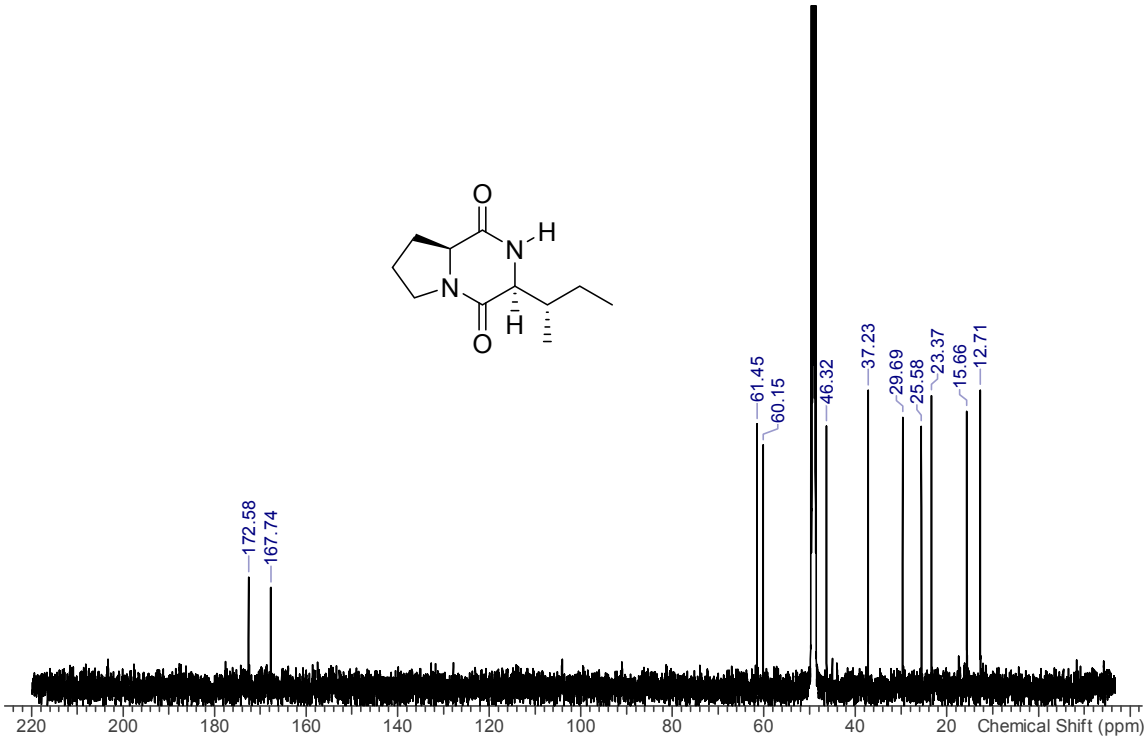


**S12.** $^{13}$C NMR spectrum (MeOH-$d_4$, 175 MHz) of *cyclo*(*S*-Pro-*S*-Ile) (**3**).

Pedras, M.; Soledade C.; Yu, Y.; Liu, J.; Tandron-Moya, Y.A. *Zeitschrift fuer Naturforschung, C: J. Biosci*. **2005**, *60*, 717–722.

**S13.** Antimicrobial assay results of compounds **1**-**3**.

**Table S13.** Antimicrobial activities of compounds **1**-**3**.

| **Strain** | **Compound 1** | **Compound 2** | **Compound 3** | **Positive control (µg/mL)** | |
|---|---|---|---|---|---|
| **Bacteria** | MIC (µg/mL) | | | | |
| *Bacillus subtilis* DSM 10 | 66.7 | - | - | 4.1 | Oxytetracyclin |
| *Chromobacterium violaceum* DSM 30191 | - | - | - | 0.4 | Oxytetracyclin |
| *Escherichia coli* DSM 1116 | - | - | - | 3.3 | Oxytetracyclin |
| *Micrococcus luteus* DSM 1790 | 66.7 | - | - | 0.2 | Oxytetracyclin |
| *Mycobacterium smegmatis* ATCC 700084 | - | - | - | 3.3 | Kanamycin |
| *Pseudomonas aeruginosa* PA14 | - | - | - | 1.7 | Gentamycin |
| *Staphylococcus aureus* DSM 346 | 66.7 | - | - | 3.3 | Oxytetracyclin |
| **Fungi** | | | | | |
| *Candida albicans* DSM 1665 | - | - | - | 66.7 | Nystatin |
| *Mucor hiemalis* DSM 2656 | 66.7 | - | - | 33.3 | Nystatin |
| *Pichia anomala* DSM 6766 | - | - | - | 33.3 | Nystatin |
| *Rhodoturula glutinis* DSM 10134 | - | - | - | 33.3 | Nystatin |
| *Schizosaccharomyces pombe* DSM 70572 | - | - | - | 33.3 | Nystatin |
| **Cell lines** | Cytotoxicity $IC_{50}$ (µg/mL) | | | | |
| KB 3.1 | 14 | - | | $5 \times 10^{-4}$ | epothilone B |
| L929 | 27 | - | | $1.1 \times 10^{-3}$ | epothilone B |

(−) no activity

**S14.** Cytotoxicity assay results of compounds **1**.

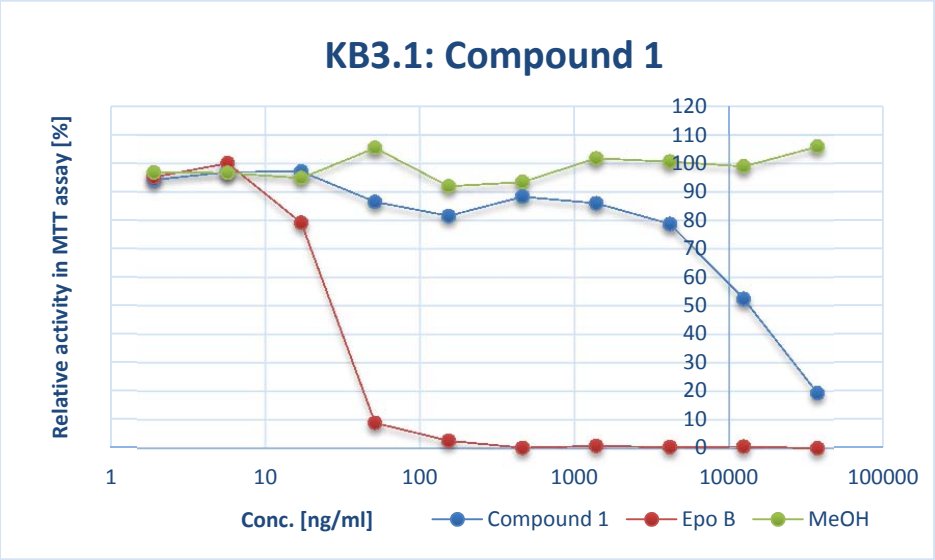


**A**

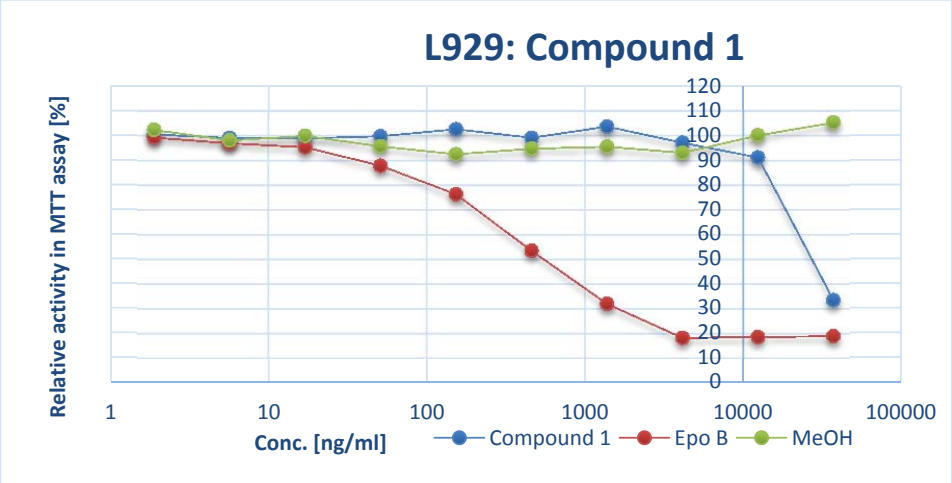


**B**

**Figure S14.** Proliferation assay. Graph of MTT assay after 5 days of incubation. *In vitro* cytotoxicity ($IC_{50}$) of compounds **1** was determined against HeLa (KB-3.1) (A) and mouse fibroblast L929 (B) cell lines. Epothilone B was used as the positive control while methanol was used as the negative control.

**S15.** Biofilm inhibitory activity of compounds **1**-**3.**

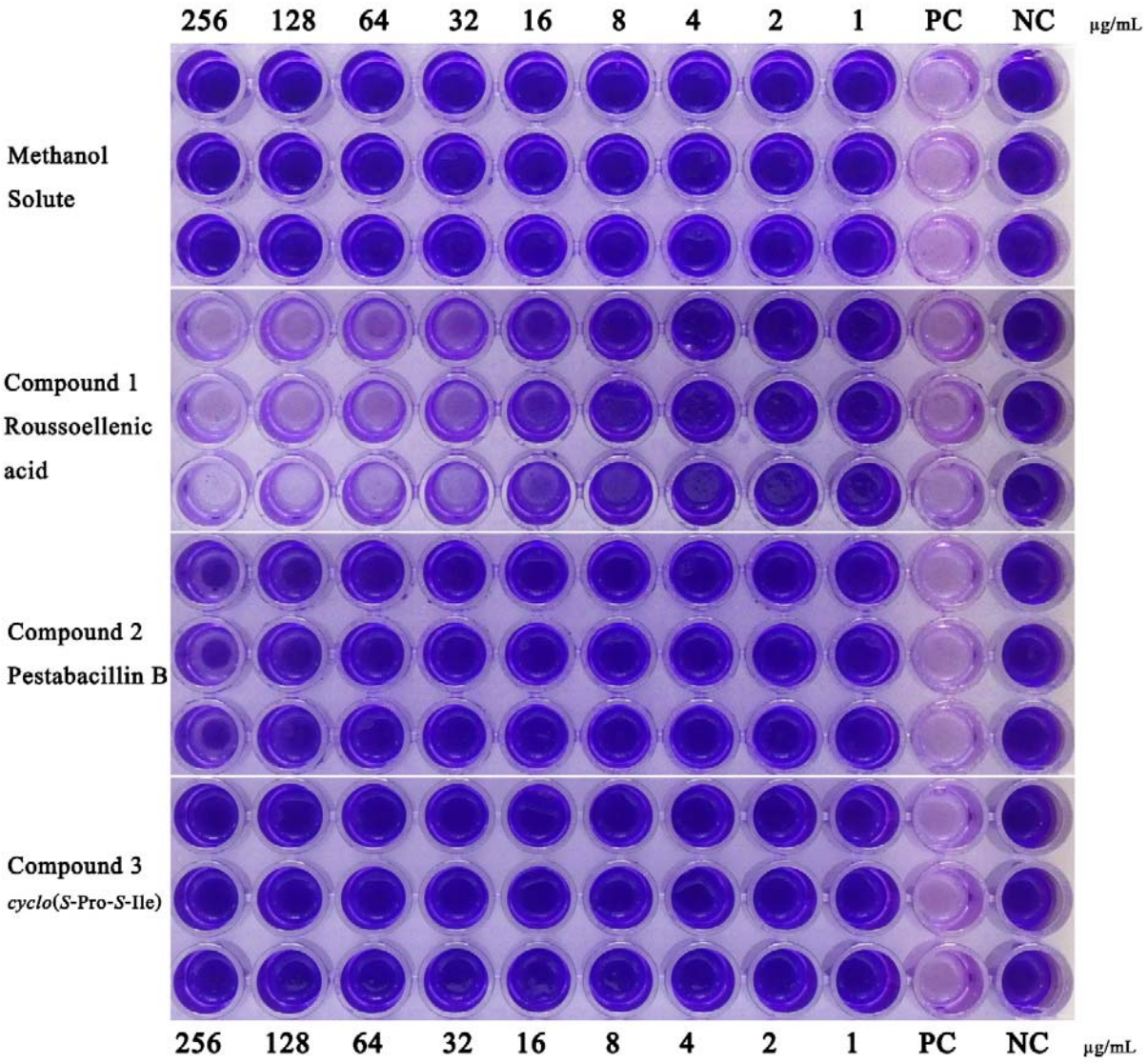


**Figure S15.** Inhibition of the biofilm formation from *Staphylococcus aureus.* CASO medium containing 4% glucose was used as the negative control and tetracycline (100 µg/mL) was used as the positive control.